Journal of Materials Chemistry A

ROYAL SOCIETY OF CHEMISTRY

PAPER

Check for updates

Cite this: *J. Mater. Chem. A*, 2022, **10**, 3093

New insights into the mechanism of cation migration induced by cation–anion dynamic coupling in superionic conductors†

Siyuan Wu,[ab] Ruijuan Xiao, *[abc] Hong Li *[abc] and Liquan Chen[abc]

Received 4th November 2021
Accepted 22nd December 2021

DOI: 10.1039/d1ta09466a

rsc.li/materials-a

Understanding the ion diffusion mechanism is one of the key preconditions for designing superionic conductors in solid state lithium batteries and many other energy devices. Besides the single-cation vacancy/interstitial-assisted and multi-cation concerted migration, the dynamic coupling between cations and anions has been detected in systems containing SO_4^{2-}, PS_4^{3-}, BH_4^-, *etc.*, and is also believed to relate to the cation migration. Here, a theory of the cation–anion interactions is presented, which classifies the coupling into *vibrational*-type and *rotational*-type according to the motion behavior of anion groups and their contributions to the ionic conductivity are analyzed. By screening the dynamic characteristics of common anion groups, a new system containing anion-assisted Li migration is identified in $LiBF_4$ and Li_2BF_5. Based on a thorough analysis of *ab initio* molecular dynamics simulations, the Li^+ migration induced by BF_4^- motion is separated from the hopping steps, and the vibration- and the rotation-assisted-migration are identified as the two characteristic processes to realize the long-range diffusion of Li^+ ions.

Introduction

Cation migration plays an important role in many devices, like solid-state lithium batteries,[1,2] fuel cells,[3] sensors,[4] and even in geophysics and geochemical[5] and planetary physics[6] *etc.* The key precondition to design a superionic material is to understand the diffusion mechanism of cations. The already confirmed factors that are closely related to cation migration in solids include atomic configurations,[7–10] free volume,[11,12] and the concerted migration mechanism,[13–17] which focus on the potential energy surface (PES) around the migrating ions geometrically or the internal interactions among a series of cations. Similarly, the dynamic coupling between anion and cation motions[18–39] has been observed by quasi-elastic neutron scattering (QENS),[23,24,28–30,34] nuclear magnetic resonance (NMR) techniques[21,22,29,31,34] or simulated by molecular dynamics[24–27,33,35–38] in some lithium or sodium superionic conductors containing anion groups such as SO_4^{2-},[18–20] PO_4^{3-},[21–23] PS_4^{3-},[24–27] $B_xH_y^{z-}$,[28–35] $XCl_6^{2/3-}$,[36] OH^- [37,38] and NO_2^-.[39] From previous experimental observations, mainly two phenomenological explanations, "paddle wheel mechanism" and "percolation mechanism", are extracted to describe how the cation migration is assisted by the motion of anion groups. Although the experimental observations provide us solid evidence on the dynamic coupling of cations and anions, it is difficult to distinguish which mechanism is the main factor or both[40] because the complex interactions between cations and anion groups are entangled and the effect of each interaction on the cation ion migration is hard to separate from the others. Through *ab initio* calculations, J. Smith *et al.* verified the coupling between the diffusing lithium ions and the rotation of anion groups from the perspective of time, space, frequency and energy for the former mechanism[26] while for the later one J. Varley *et al.* expanded the lattice parameters of $Li_2B_{12}H_{12}$ to verify that lattice expansion is the key to the ion diffusion.[33] However, it still puzzles us that why both of them belonging to thermophoresis will be coupling rather than competing. If both of them are in the nonequilibrium state, it sounds contradictory as it has been detected at the same time by experiments. It must be the situation which they suppress each other. Therefore there exist the following questions remaining to be solved. *e.g.*, How many modes exist in the dynamic coupling between cations and anion groups?, how each mode affects the cation migration?, in which situation the coupling promotes the diffusion behavior?, how to look for or design superionic materials assisted by cation–anion interactions? and what is the image for each mode?

The first step to clarify above questions is to understand the motions of anion groups. In theoretical simulations, such as semi-empirical energy barrier evaluation[41,44,45] or *ab initio* molecular dynamics[46] (AIMD), the kinetic motion of anion groups and its effect on changing the PES can be considered mode by mode, providing an efficient tool to decompose the

[a]*Beijing Advanced Innovation Center for Materials Genome Engineering, Institute of Physics, Chinese Academy of Sciences, Beijing 100190, China. E-mail: rjxiao@iphy.ac.cn; hli@iphy.ac.cn*

[b]*School of Physical Sciences, University of Chinese Academy of Sciences, Beijing, 100049, China*

[c]*Yangtze River Delta Physics Research Center Co. Ltd, Liyang 213300, China*

† Electronic supplementary information (ESI) available. See DOI: 10.1039/d1ta09466a

average and comprehensive effects observed in QENS and NMR experiments. Here, by adopting atomic simulation methods, we introduce a simple and efficient model to characterize the cation migration induced by dynamic coupling with anion groups, in which the motion behavior of the anion groups is classified into *vibrational*-type and *rotational*-type and its contributions to the ionic conductivity are analyzed. Furthermore, we suggest a lithium ionic conductor system evolved cation–anion dynamic coupling through the BF_4^- group, and two detailed *rotational*-type processes related to the *intra*-ring mode and *inter*-bridge mode are identified through AIMD simulations. The close frequencies or velocities between the coupled anion and cation are the necessary conditions for improving the diffusion of cations. These understandings unlock efficient ways to design superionic conductors with improved kinetic properties enhanced by dynamic coupling between cations and anion groups, and provide additional physical insight into the superionic behavior.

Results and discussion

Motion of anion groups

To get prima facie common features of the systems evolved in the anion-assisted cation migration, we sort out the motion ability of anion groups which show positive effects on the diffusion of cations.[18–39] All the ions contained in these compounds can be classified into three types according to their functions in the ion transport process. The immobile cations act as the framework to stabilize the structure. The anions bind with the immobile cations to form various polyhedra and the immobile cations act as the center for anions to vibrate or rotate. The mobile cations, *e.g.*, Li^+ or Na^+, diffuse along the channels within the framework constructed by the immobile cations and anions. In the anion-assisted migration mechanism, the dynamic coupling refers to the interaction between anions and mobile cations and it is believed that the movement of anions in a small range will promote the surrounding Li^+ or Na^+ ions to migrate among lattice sites. To measure the motion ability of anions, the bond-valence simulations[41,44,45] are carried out to calculate the energy barriers, E_{rot} and E_{mig}, for the anions to rotate within one group and migrate between neighboring groups respectively. When the driving forces are less than E_{rot}, the main movement mode of the anion groups is vibration, as illustrated in Fig. 1(d) and shown as the red part in Fig. 1(a). If the driving forces are larger than E_{rot} but less than E_{mig} (the cyanine part in Fig. 1(a)), the rotation of the anion groups, indicated in Fig. 1(c), will be stimulated. The migration of anions from the lattice site within one group to another as shown in Fig. 1(b) only happens when the driving forces are larger than E_{mig} and the migration of anions between the lattice sites of different groups is an indicator of anion conductor behavior, which is beyond discussion of our current work.

As shown in Fig. 1(a), very similar values of E_{rot} can be found for the same type of anion groups, which obeys the intuition since the rotation behavior is mainly related to the rotational inertia and determined by the local structure of the anion group

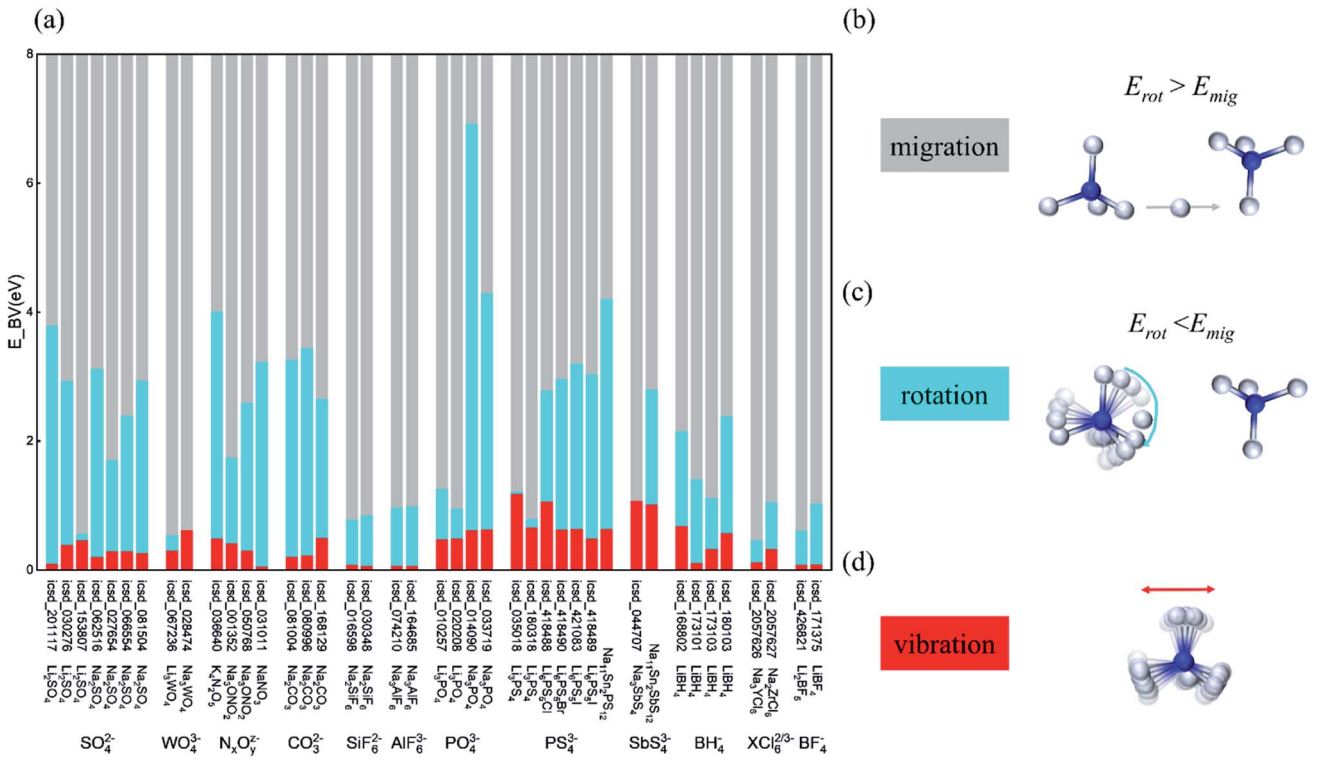

Fig. 1 (a) The rotation and migration energy barriers, E_{rot} and E_{mig}, estimated by bond-valence simulations for the anions in materials from ref. 18–39; (b)–(d): diagrammatic figures for the migration-, rotation- and vibration-movement modes of anions. In BV simulation, we infer rotation as atom forming the connecting path in the same group which may be a little different in AIMD. More details in the Methods section and Table S1 in the ESI.†

 This journal is © The Royal Society of Chemistry 2022

itself, while the values of E_{mig} are distributed in a relatively large range even for the same anion group because various arrangements of anion groups exist in different compounds such as the two Li_3PO_4 isomers shown in Fig. S1.† For most structures illustrated in Fig. 1(a), the much higher cyanine bar compared to the red one means migration is more difficult than rotation, indicating that the anion induces the cation motion mainly by its rotation, as shown in Fig. 1(c) for the BH_4^- group in ref. 31, SO_4^{2-} group in ref. 21 and Li_3PO_4 shown in Fig. S1.† However, for WO_4^{3-} and XS_4^{3-} (X = P, Sb), similar E_{mig} and E_{rot} are found implying that the rotation of the group is difficult to be triggered. Thus the vibration mode as shown in Fig. 1(d) is the major way for the interplay between anions and mobile cations. This is consistent with the evidence provided in ref. 18, in which WO_4^{3-} replaced SO_4^{2-} and enhanced the diffusion of Li^+ without rotation and the same as in XS_4^{3-} (X = P, Sb) in ref. 24 and 27. It also clarifies the contradiction shown in ref. 26 and 33, $B_{12}H_{12}^{2-}$ can rotate easily especially expanding the lattice while PS_4^{3-} seems to vibrate at low temperatures. According to above analysis, the comparison between E_{mig} and E_{rot} can be used as the first rule to judge in which mode the anions and mobile cations couple dynamically. If the part of rotation is much larger than the part of vibration, it has more chances to rotate. Some clues for distinguishing the main coupling mode are hidden in the structural information. For example, in anti-perovskite Na_3ONO_2 (icsd_001352 and icsd_050768),[39] the partial occupation of O^{2-} anions at sites within the NO_2^- group implies that lots of local minimum exist on the PES around N^{3+} and the barrier for the rotation of the NO_2^- group is very small as shown in Fig. 1(a), thus the dynamic coupling between cations and anion groups is mainly through the *rotational*-type. However in Li_3PS_4 (icsd_035018), large values of the isotropic atomic displacement parameters are found for the S^{2-} anions which implies that these ions vibrate around the equilibrium site with a relatively large amplitude, thus the vibration mode is the major coupling way between Li^+ and PS_4^{3-} groups.

Mechanism of anion group assisted Li^+ diffusion

For the two coupling methods based on *vibrational*- and *rotational*-type, their effects on cation migration are analyzed as illustrated in Fig. 2, in which an anion group with four-coordinated environment is taken as an example. For the coupling through *vibrational*-type mode of anions, the simple harmonic vibration is assumed to simplify the understanding of its effect on the cation migration and the varied amplitude of the cation ion is deduced in the ESI† and taken as the indicator of the change of its migration ability since the larger the amplitude of cation vibration, the easier for the cation to diffuse[42,43] as shown in Fig. 2(a). Besides, the amplitude of cation vibration also reflects the difficulty of breaking and making the cation–anion bond during the migration process through the antisymmetric stretching vibration.

Two cases are considered according to the direction of cation/anion vibration and the schematic diagrams are shown in Fig. 2(b) and (c). Eqn (1) and (2) express the new amplitude (A'_c) of the mobile cation under the dynamic coupling through the anion vibration perpendicular and parallel to the migration direction of the cation, in which A_c, A_a, φ_c, φ_a, ω_c and ω_a are the amplitude, phase position and frequency of the mobile cation and anion without coupling, respectively. For the perpendicular situation expressed in eqn (1), $A'_c$is always larger or not smaller than A_c indicating that the cation migration is invariably enhanced and the direction of the cation migration is also changed. For the parallel mode expressed in eqn (2) the situation is much more complex. One way to ensure $A'_c > A_c$ is to under the condition of $A_a > 2A_c$, however, the much larger amplitude of the anion vibration might indicate that the material is likely to be an anion conductor or it is easy for the

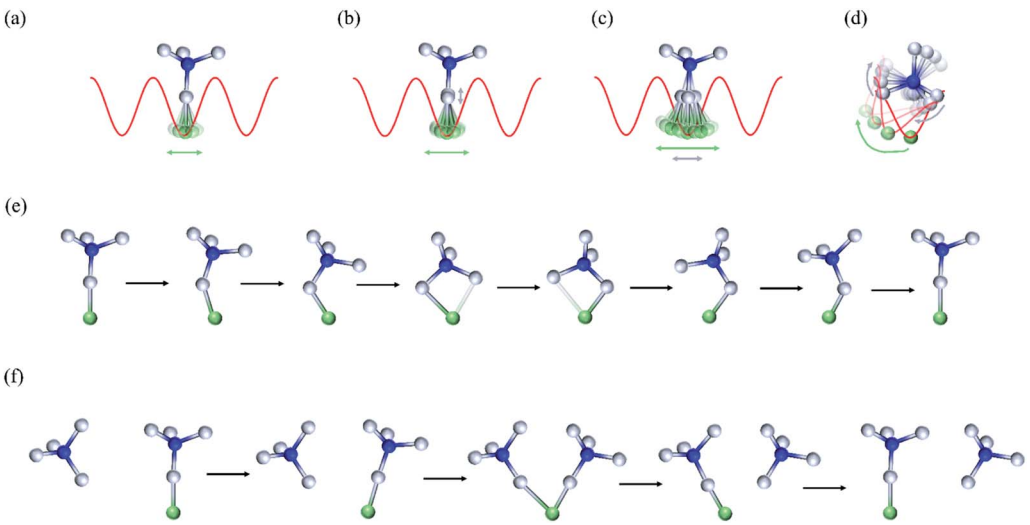

Fig. 2 The mode-by-mode analysis of the effects of cation–anion dynamic coupling on cation migration. (a) The migrating cation vibrates at the balance site in the assumption of the simple harmonic way without any coupling between the cation and anion; (b) the perpendicular-situation and (c) the parallel-situation for the *vibrational*-type coupling; (d) the situation for the *rotational*-type coupling. (e) and (f) are the diagrammatic figures for *intra*-ring mode and *inter*-bridge mode respectively.

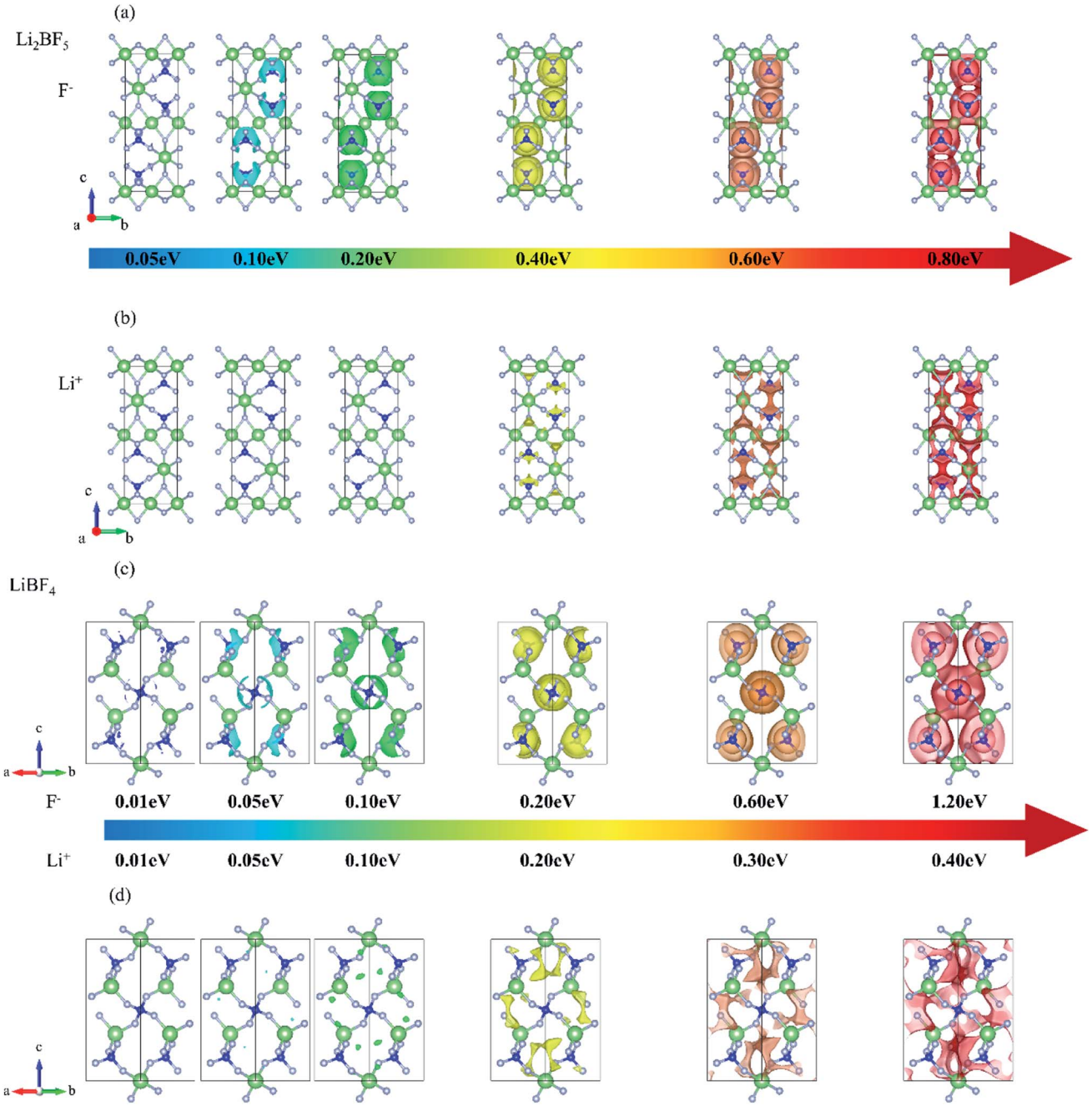

Fig. 3 The potential energy isosurfaces of (a) the F^- anions and (b) the Li^+ cations at 0.05 eV, 0.10 eV, 0.20 eV, 0.40 eV, 0.60 eV and 0.80 eV in Li_2BF_5. (c) the potential energy isosurfaces of F^- in $LiBF_4$ at 0.01 eV, 0.05 eV, 0.10 eV, 0.20 eV, 0.60 eV and 1.20 eV and (d) the potential energy isosurfaces of Li^+ in $LiBF_4$ at 0.01 eV, 0.05 eV, 0.10 eV, 0.20 eV, 0.30 eV and 0.40 eV. Green, blue and light gray spheres represent the Li, B and F atoms respectively.

anion to leave its equilibrium site and transform from the vibrational coupling mode into the rotational one as discussed later. Another possibility is that the phase position satisfies eqn (3) if the frequencies are the same or the time interval, Δt, between two diffusion events satisfies eqn (4) if the frequencies are different. Details are shown in eqn S8–S13† and we can conclude that the close frequencies between anions and migrating cations benefit the diffusion of cations.

$$A'_c = \sqrt{\frac{(A_c^2 + A_a^2) + \sqrt{(A_c^2 - A_a^2)^2 + 4A_cA_a\cos^2[(\omega_c - \omega_a)t + (\varphi_c - \varphi_a)]}}{2}} \quad (1)$$

This journal is © The Royal Society of Chemistry 2022

$$A'_c = \sqrt{A_c^2 + A_a^2 + 2A_cA_a\cos[(\omega_c - \omega_a)t + (\varphi_c - \varphi_a)]} \quad (2)$$

$$|\varphi_c - \varphi_a| < \arccos\left(-\frac{A_a}{2A_c}\right) \quad (3)$$

$$\Delta t < \frac{2\arccos\left(-\frac{A_a}{2A_c}\right)}{|\omega_c - \omega_a|} \quad (4)$$

However, if the dynamic coupling is realized by the anion group rotation mode, the simple harmonic vibration is invalid since the anions will leave the equilibrium site and move to another site within the same anion group. In this case, the rotation of the anion group changes the PES nearby and the original site cation lying is not the one with the minimum energy anymore, thus it has the tendency to look for the new stable site along with the rotation of the anion group as shown in Fig. 2(d). The migration of cations can be divided into *intra*-ring mode and *inter*-bridge mode according to their destination sites. In the former one, the mobile cation migrates but still bonds with the anion in the same group (as shown in Fig. 2(e)), while in the later one, the diffusing cation breaks the bond with the anion and moves towards another anion group to form the new chemical bond between the anion and the cation itself (as shown in Fig. 2(f)). The later analysis on the detailed migration process through AIMD will show that the close velocities between the coupled anions and cations are beneficial for diffusion. It is obvious that the *inter*-bridge mode is the key process for mobile cations to form a long-range migration pathway through the bulk of the material. According to the above analysis, the anion mobility expressed by E_{mig} and E_{rot} determines the coupling mode between anion groups and diffusing cations, and the close frequencies or velocities and larger fluctuations of anion groups are beneficial for the cation migration.

Finding new systems: $LiBF_4$ and Li_2BF_5

Based on the above understanding, the previously undiscovered systems with anion–cation dynamic coupling can be found. Two of them are the compounds with the BF_4^- group, *e.g.*, $LiBF_4$ and Li_2BF_5. Different arrangements of Li^+ and BF_4^- exist in them and the strong interaction between Li^+ and F^- is expected to affect the diffusion of Li^+. The energy barriers for the BF_4^- group to rotate or migrate in Li_2BF_5 and $LiBF_4$ are shown in Fig. 3, in which a series of isopotential surfaces for Li^+ and F^- are estimated by the bond-valence method.[41,44,45] In Li_2BF_5 the motion of F^- changes from vibration around the original site with a small value to form isopotential surface (smaller than 0.20 eV) to rotation around the central ion (B^{3+}) with a medium value to form isopotential surface (0.20–0.60 eV) and diffusion as a diffusion net across the lattice cell with a high value to form isopotential surface (larger than 0.60 eV). Different from F^-, no rotation mode is found for Li^+ and only the vibration around the origin site and the migration across the lattice site are identified. The same results are presented by $LiBF_4$ except that they have different critical energies.

Although the bond-valence simulations give the tendency of the movement ability of anions, the real anion motion cannot be introduced in the model for the diffusion of cations,[44] therefore the AIMD simulations[46] are performed to further obtain the detailed picture of Li^+ migration assisted by the dynamic coupling with BF_4^- anion groups. We carry out the AIMD simulations for $LiBF_4$ and Li_2BF_5 at 600 K for 50 and 60 ps, respectively, with a time step of 1 fs. We focus on the variation of the following four quantities during the kinetic process, including the displacement of the Li^+ ion, the length of the B–F bond, the distance between neighboring Li^+ and F^- ions and the rotation angle of the B–F bond (see Methods in the ESI†). Firstly the diffusion events within the two systems and their occurrence of the time periods are picked out by analyzing the displacement of each Li^+ ion as illustrated in Fig. S2(a) and (b),† in which four diffusion events are identified in Li_2BF_5 and one in $LiBF_4$. These events can be classified into two types according to the coupling mode. Secondly the above four quantities and their variations are analyzed for the different types of migration processes, including the vibration-assisted diffusion for the 25th Li^+ ion in Li_2BF_5 during 44–46 ps, the mixed *vibration*- and interstitial-assisted processes for the 24th Li^+ ion in Li_2BF_5 during 44–47 ps and the *rotation*-assisted diffusion for the 8th Li^+ ion in $LiBF_4$ during 30–40 ps. Besides, the 4th Li^+ ion in Li_2BF_5 during 45–55 ps and the 8th Li^+ ion in $LiBF_4$ during 0–10 ps are also analyzed for comparison. The detailed results are shown in Fig. S3–S8 and the ESI.† In all the cases, the length of the B–F bond almost remains constant around 1.4 Å indicating that no breaking of the B–F bond happens and the BF_4^- groups are stable. The length of the Li–F bond will remain ~2 Å if the Li^+ ion moves nearby. Either the vibration or the rotation mode of BF_4^- groups is observed according to the rotation angle of the B–F bond. The autocorrelation function (AF), expressed in eqn (5), is adopted to understand the relationship between the cation and anion and shown in Fig. S6.†

$$AF = \sum \frac{\langle \theta(t)\theta(t+t')\rangle}{\langle \theta(t)\theta(t)\rangle} \quad (5)$$

The migration of the 25th Li^+ (Li25) in Li_2BF_5 as shown in Fig. 4(a) is assisted by the vibration of F^- ions around it. The anions within the four BF_4^- groups around Li25 only vibrate around the original sites as shown in Fig. 4(a). The AF of Li25–F24–B7 and Li25–F41–B12 as shown in Fig. S6(a)† almost remaining constant during the diffusion confirms the correlation between them and provides evidence of the close frequencies between Li^+ and F^-. The diffusion of Li24 is divided into two sections which mixed *vibration*- and interstitial-assisted processes and Li^+ will diffuse into an interstitial site first and stay there to rest then through the vibrational mode it finishes the migration process as shown in Fig. 4(b) and S4.† The AF shown in Fig. S6(b)† also proves it. These processes are similar to passing a football between athletes (F^- anions) who stand at the fixed sites. The rotation mode of the BF_4^- group is found in the 8th Li^+ ion in $LiBF_4$ (Fig. 4(c)). It experiences the *inter*-bridge mode diffusion as shown in Fig. S5,† however for

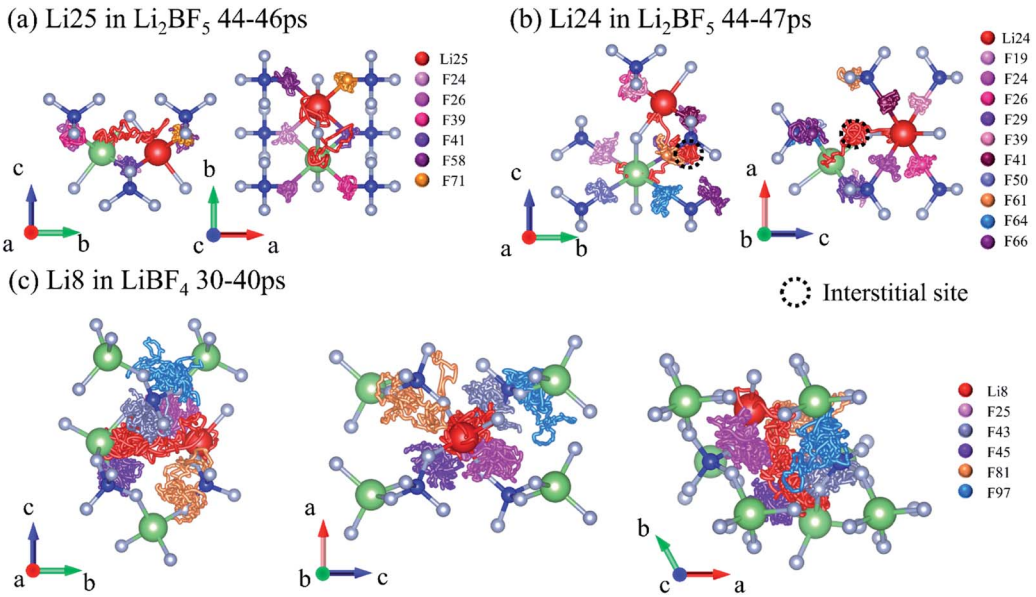

Fig. 4 The trajectories for (a) 25th Li^+ and F^- in Li_2BF_5 in 44–46 ps from the view of the *a* axis and *c* axis, (b) 24th Li^+ and F^- in Li_2BF_5 in 44–47 ps from the view of *a* axis and *b* axis (c) 8th Li^+ and F^- in $LiBF_4$ in 30–40 ps from the view of *a*, *b* and *c* axes. Green, blue and light gray spheres represent the Li, B and F atoms respectively.

the same Li^+ the *intra*-ring mode is also found during 0–10 ps as illustrated in Fig. S7.† As shown in Fig. S5† especially (b), (j) and (n), the motion of the cation catches up with the rotation of the anion group (the movement of Li^+ and the rotation angle of BF_4^- are changing simultaneously but the distance between Li^+ and F^- remains constant), and the *inter*-bridge mode is formed which can be viewed as the situation that one running athlete controls the football and passes it to another athlete as shown in Fig. 2(f). While the constant distance between Li^+ and F^- implies the close velocities of the coupled ions, it is regarded as the condition to increase the cation migration through the *rotational*-coupling mode. The situation shown in Fig. S7† especially (a) and (d) is that the running athlete fails in controlling the football and leaves it where it is as shown in Fig. 2(e). And there doesn't exist correlation between the cation and anion as shown in Fig. S6(c).† For the 4th Li^+ in Li_2BF_5, it can also be divided into two diffusion sections during 45–55 ps. As shown in Fig. 5(a) and S8,† it has a rest at an interstitial site during diffusion (black dotted circle in Fig. 5(a)). For the front part (46–47 ps), it clearly appears the rotation of BF_4^- and the

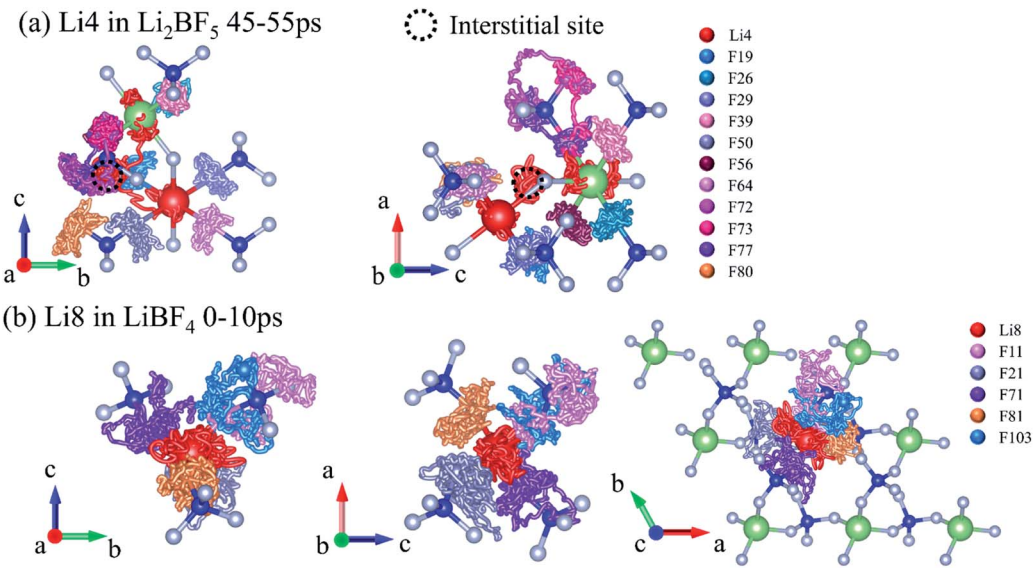

Fig. 5 The trajectories for (a) the 4th Li^+ and F^- in Li_2BF_5 in 45–55 ps from the view of the *a* axis and *b* axis, (b) the 8th Li^+ and F^- in $LiBF_4$ in 0–10 ps from the view of *a*, *b* and *c* axes. Green, blue and light gray spheres represent the Li, B and F atoms respectively.

 This journal is © The Royal Society of Chemistry 2022

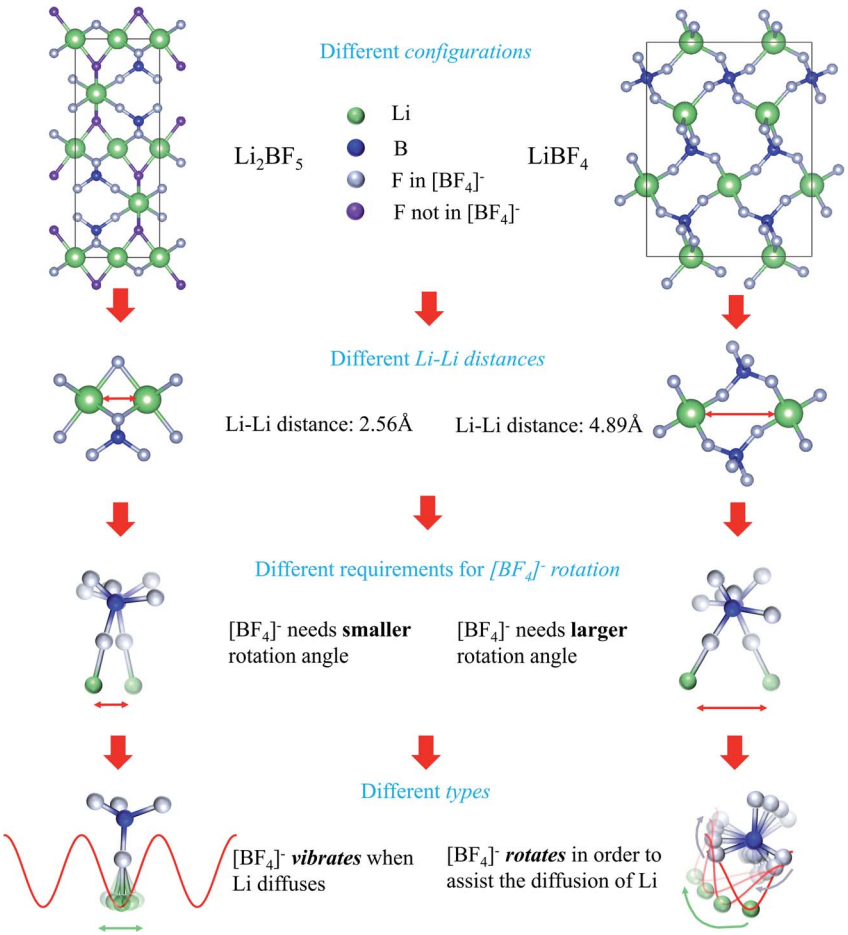

Fig. 6 Discrepancies in $LiBF_4$ and Li_2BF_5. In Li_2BF_5 the smaller distance between Li atoms reveals that it only needs a smaller rotation angle while it is opposed in $LiBF_4$.

angle is 120° (Fig. S8(j)–(l)†). However there exists about 0.5 ps hysteresis for the rotation which can also be captured in the autocorrelation function shown in Fig. S6(d).† During 47–53 ps it seems Li vibrates at this interstitial site (in Fig S8† we can see the black line referred to the displacements of Li exists a platform between 47–53 ps which is corresponding to the red cluster circled in the black dotted circle in Fig. 5(a)). The back part (53–55 ps) is short diffusion and it is similar to Li25 during 44–46 ps. The same as in 8th Li^+ in $LiBF_4$ with no diffusion of Li^+ as shown in Fig. S6(c) and S7,† the BF_4^- rotates as 120° (red line in Fig. S7(a), (b), (d), (e), (f) and (h)† shows the rotaion of BF_4^-) while there is no diffusion for Li^+ (black line in Fig. S7† shows no diffusion for Li). So vibration/rotation of the anion is not the sufficient condition for diffusion of the cation. As shown before, local adjustments especially rotation of the anion group will reduce the electrostatic interaction so the rotation of the anion is a necessary condition for diffusion of the cation but does not always promote it. Although the real situation is much more complex because it is the comprehensive effect of all the above modes, a relatively clear picture of BF_4^- anion-assisted Li^+ migration still can be extracted for the two systems. For $LiBF_4$, the vibration of F^- enhances the vibration of Li^+ while the rotation of the BF_4^- group provides help for the diffusion of Li^+ among the lattice and interstitial sites due to the large distance (4.89 Å in Fig. 6) between two sites. For Li_2BF_5, the vibration of F^- promotes the Li^+ diffusion along the *ab* plane while the interstitial-assisted with the vibration of F^- induces the diffusion of Li^+ across the *ab* plane and forms a long-range migration pathway. In fact, the division between the *vibration*- and *rotation*-assisted migrations is based on the average excursion and to some extent they show a similar origin and here we distinguish it according to the changes of the PES. The vibration/rotation is one of the intrinsic behaviors of anion groups and not the sufficient but necessary condition for diffusion of the cation. Whether the "paddle wheel mechanism" or "percolation mechanism" is the part process of the interaction between cations and anion groups, if only 0–10 ps in $LiBF_4$ or 44–55 ps for Li4 in Li_2BF_5 is observed, the conclusion will be that the volume is the key factor while if 30–40 ps in $LiBF_4$ or 44–47 ps for Li24/25 in Li_2BF_5 is analyzed, the conclusion is that the rotation is along with diffusion will be reached. We should focus more on the effects of each single coupling mode on the cation migration rather than the average results. Last but not least we must emphasize that in fact the discrepancy between *vibrational*-type and *rotational*-type is does not exist (more discussions in the ESI†). We cannot divide these continuous

variations into two separate parts absolutely and we classify these, which have no effect on the PES of the cation, into the *vibrational*-type and others into the *rotational*-type. Although in BV we can easily divide it, it becomes more difficult in AIMD. So here in AIMD we refer rotation as the rotation angle during diffusion is larger than that during no diffusion. For Li_2BF_5, even though Li^+ diffuses or not, the rotation of BF_4 exhibits no obvious change so we considered it as *vibrational*-type. For $LiBF_4$, we can observe the rotation of BF_4 with the diffusion of Li^+ so we assume that it is *rotational*-type. But as shown in Fig. 6, the smaller distance between Li ions in Li_2BF_5 indicates that it has little dependence on the rotation of anion groups (BF_4^- rotation at a smaller angle can ensure the diffusion of Li) while it is different in $LiBF_4$ where a larger distance between Li atoms indicates that it needs a larger rotation angle.

Conclusions

In summary, the anion-assisted cation migration is one of the diffusion mechanisms in superionic conductors as important as the vacancy/interstitial- or the concerted-migration mechanism. By evaluating the movement ability of anions in a substantial number of structures, the dynamic coupling of anions and migrating cations is classified into *vibrational*- and *rotational*-type according to their effects on the PES, and their effects on the cation migration are analyzed mode by mode. It is identified that the close frequencies between the anion group and migrating cation or the large vibration amplitude of anions are required to assist the cation migration in the vibration coupling mode, while the close velocities between anions and cations are the conditions to realize the *inter*-bridge migration in long-range pathways in *rotational*-type. In the cases where the cation–anion dynamic coupling plays an important role, we understand that vibration/rotation of the anion is not the sufficient but a necessary condition for diffusion of the cation. Based on the effects of anion groups, a new system with the BF_4^- group is identified as a candidate in which the anion-assisted phenomenon will be obvious. $LiBF_4$ and Li_2BF_5 are taken as the model structures to evaluate the effect. A detailed analysis of the AIMD simulation reveals all the vibration-assisted-migrations and rotation-assisted-migrations, including both the *intra*-ring mode and *inter*-bridge mode, in the hopping steps of the two compounds. These understandings provide a new horizon to look for and design superionic conductors, as well as develop the insight about the ionic transport phenomenon.

Conflicts of interest

There are no conflicts to declare.

Acknowledgements

We acknowledge the National Natural Science Foundation of China (grant number 52022106 and 51772321) for financial support, and Tianjin Supercomputer Center for providing computing resources.

References

1 M. Armand and J. Tarascon, *Nature*, 2018, **451**, 652–657.
2 J. Tarascon and M. Armand, *Nature*, 2001, **414**, 359–367.
3 N. Minh, *J. Am. Ceram. Soc.*, 1993, **76**, 563–588.
4 E. Traversa, *Sens. Actuators, B*, 1995, **23**, 135–156.
5 B. Zhang, X. Guo, T. Yoshino and Q. Xia, *Natl. Sci. Rev.*, 2021, nwab064, DOI: 10.1093/nsr/nwab064.
6 M. Millot, F. Coppari, J. Ryan Rygg, A. Correa Barrios, S. Hamel, C. Swift and H. Eggert, *Nature*, 2019, **569**, 251–255.
7 Z. Rong, R. Malik, P. Canepa, G. Gautam, M. Liu, A. Jain, K. Persson and G. Ceder, *Chem. Mater.*, 2015, **27**, 6016–6021.
8 Y. Wang, W. Richards, S. Ong, L. Miara, J. Kim, Y. Mo and G. Ceder, *Nat. Mater.*, 2015, **14**, 1026–1031.
9 P. Canepa, S. Bo, G. Gautam, B. Key, W. Richards, T. Shi, Y. Tian, Y. W. J. Li and G. Ceder, *Nat. Commun.*, 2019, **8**, 1759.
10 Z. Xu, X. Chen, R. Chen, X. Li and H. Zhu, *npj Comput. Mater.*, 2020, **6**, 47.
11 B. He, S. Chi, A. Ye, P. Mi, L. Zhang, B. Pu, Z. Zou, Y. Ran, Q. Zhao, D. Wang, W. Zhang, J. Zhao, S. Adams, M. Avdeev and S. Shi, *Sci. Data*, 2020, **7**, 151.
12 J. Peng, Y. Liu, Y. Pan, J. Wu, Y. Su, Y. Guo, X. Wu, C. Wu and Y. Xie, *J. Am. Chem. Soc.*, 2020, **142**, 18645–18651.
13 R. Jalem, Y. Yamamoto, H. Shiiba, M. Nakayama, H. Munakat, T. Kasuga and K. Kanamura, *Chem. Mater.*, 2013, **25**, 425–430.
14 K. Meier, T. Laino and A. Curioni, *J. Phys. Chem. C*, 2014, **118**, 6668–6679.
15 M. Burbano, D. Carlier, F. Boucher, B. Morgan and M. Salanne, *Phys. Rev. Lett.*, 2016, **116**, 135901.
16 M. Xu, J. Ding and E. Ma, *Appl. Phys. Lett.*, 2012, **101**, 031901.
17 X. He, Y. Zhu and Y. Mo, *Nat. Commun.*, 2017, **8**, 15893.
18 E. Secco, *Solid State Commun.*, 1988, **66**, 921–923.
19 A. Campbell, K. MacDonald and E. Secco, *J. Solid State Chem.*, 1989, **81**, 65–69.
20 E. Secco, *Solid State Ionics*, 1988, **28–30**, 168–172.
21 M. Witschas and H. Eckert, *J. Phys. Chem. A*, 1999, **103**, 10764–10775.
22 M. Witschas, H. Eckert, H. Freiheit, A. Putnis, G. Korus and M. Jansen, *J. Phys. Chem. A*, 2001, **105**, 6808–6816.
23 D. Wilmer, H. Feldmann and R. Lechner, *Phys. Chem. Chem. Phys.*, 2002, **4**, 3260–3265.
24 Z. Zhang, P. Roy, H. Li, M. Avdeev and L. Nazar, *J. Am. Chem. Soc.*, 2019, **141**, 19360–19372.
25 S. Adams and R. Raoa, *J. Mater. Chem.*, 2012, **22**, 7687–7691.
26 J. Smith and D. Siegel, *Nat. Commun.*, 2020, **11**, 1483.
27 Z. Zhang, H. Li, K. Kaup, L. Zhou, P. Roy and L. Nazar, *Matter*, 2020, **2**, 1667–1684.
28 N. Verdal, T. Udovic, V. Stavila, W. Tang, J. Rush and A. Skripov, *J. Phys. Chem. C*, 2014, **118**, 17483–17489.
29 T. Udovic, M. Matsuo, W. Tang, H. Wu, V. Stavila, A. Soloninin, R. Skoryunov, O. Babanova, A. Skripov, J. Rush, A. Unemoto, H. Takamura and S. Orimo, *Adv. Mater.*, 2014, **26**, 7622–7626.
30 W. Tang, M. Matsuo, H. Wu, V. Stavila, W. Zhou, A. Talin, A. Soloninin, R. Skoryunov, O. Babanova, A. Skripov,

 This journal is © The Royal Society of Chemistry 2022

A. Unemoto, S. Orimo and T. Udovic, *Adv. Energy Mater.*, 2016, **6**, 1502237.
31 M. Matsuo and S. Orimo, *Adv. Energy Mater.*, 2011, **1**, 161.
32 T. Udovic, M. Matsuo, A. Unemoto, N. Verdal, V. Stavila, A. Skripov and J. Rush, *Chem. Commun.*, 2014, **50**, 3750–3752.
33 J. Varley, O. Kweon, P. Mehta, P. Shea, T. Heo, J. Terrence, T. Udovic, V. Stavila and B. Wood, *ACS Energy Lett.*, 2017, **2**, 250–255.
34 W. Tang, A. Unemoto, W. Zhou, V. Stavila, M. Matsuo, H. Wu, S. Orimo and T. Udovic, *Energy Environ. Sci.*, 2015, **8**, 3637–3645.
35 Z. Lu and F. Ciucci, *J. Mater. Chem. A*, 2016, **4**, 17740–17748.
36 E. Wu, S. Banerjee, H. Tang, P. Richardson, J. Doux, J. Qi, Z. Zhu, A. Grenier, Y. Li, E. Zhao, G. Deysher, E. Sebti, H. Nguyen, R. Ste-phens, G. Verbist, K. Chapman, R. Clément, A. Banerjee, Y. Meng and S. Ong, *Nat. Commun.*, 2021, **12**, 1256.
37 J. Howard, Z. Hood and N. Holzwarth, *Phys. Rev. Mater.*, 2017, **1**, 075406.
38 A. Soon, Y. Xiao, K. Turcheniuk, P. Upadhya, A. Ramanujapuram, J. Benson, A. Magasinski, M. Olguin, L. Meda, O. Borodin and G. Yushin, *Adv. Energy Mater.*, 2018, **8**, 1700971.
39 L. Gao, H. Zhang, Y. Wang, S. Li, R. Zhao, Y. Wang, S. Gao, L. He, H. Song, R. Zou and Y. Zhao, *J. Mater. Chem. A*, 2020, **8**, 21265–21272.
40 M. Jansen, *Angew. Chem., Int. Ed.*, 1991, **30**, 1547–1558.
41 R. Xiao, H. Li and L. Chen, *Sci. Rep.*, 2015, **5**, 14227.
42 S. Muy, J. Bachman, L. Giordano, H. Chang, D. Abernathy, D. Bansal, O. Delaire, S. Hori, R. Kanno, F. Maglia, S. Lupart, P. Lamp and S. Yang, *Energy Environ. Sci.*, 2018, **11**, 850–859.
43 K. Wakamura, *Phys. Rev. B: Condens. Matter Mater. Phys.*, 1997, **56**, 11593.
44 S. Adams and R. P. Rao, *Phys. Status Solidi A*, 2011, **208**, 1746.
45 R. Xiao, H. Li and L. Chen, *Journal of Materiomics*, 2015, **1**, 325.
46 X. He, Y. Zhu, A. Epstein and Y. Mo, *npj Comput. Mater.*, 2018, **4**, 18.